

A New Homologous Series $\text{Sr}_{n-1}\text{Cu}_{n+1}\text{O}_{2n}$ Found in the SrO–CuO System Treated under High Pressure

Z. HIROI,* M. AZUMA, M. TAKANO, AND Y. BANDO

Institute for Chemical Research, Kyoto University, Uji, Kyoto-fu 611, Japan

Communicated by J. M. Honig, August 20, 1991

A new homologous series of high-pressure phases, $\text{Sr}_{n-1}\text{Cu}_{n+1}\text{O}_{2n}$ ($n = 3, 5, \dots$), were found in the SrO–CuO system treated at 6 GPa and 1373–1573 K. These crystallize in orthorhombic structures of space group *Cmmm* with unit-cell parameters of $a \sim 3.9 \text{ \AA}$, $b \sim n \times a$, and $c \sim 3.5 \text{ \AA}$. Along the *c*-axis $\text{Cu}_{1+1/n}\text{O}_2$ sheets alternate with $\text{Sr}_{1-1/n}$ sheets without oxygen. Within the Cu–O sheets, Cu–O double chains made of corner- and edge-sharing CuO_4 squares are intergrown with a corner-sharing CuO_4 network; the distance between the double chains is $b/2$. The serial chemical composition and structure are interpreted as resulting from a shear operation upon the high-pressure form of SrCuO_2 ($n = \infty$). © 1991 Academic Press, Inc.

Introduction

Cupric oxide superconductors are not simple oxides made of Cu–O bonds only, but are complex oxides containing counter cations (c.c.) also that compensate the negative charge of the CuO_2 sheets. Since the Cu–O and the c.c.–O bonds should have different compressibilities and different thermal expansion coefficients from each other, synthesis in various pressure–temperature regions may be expected to yield new phases. We have studied high-pressure effects upon alkaline-earth (A)- and rare-earth Ln –Cu–O systems (1, 2) and have found superconductivity in the A–Cu–O system treated at 6 GPa (3, 4). It should be noticed that this system is free from trivalent and quadrivalent c.c.’s like rare-earth ions,

Bi^{3+} or Tl^{3+} , which are indispensable to superconducting phases found at ambient pressure. The superconductor’s structure is based on the so-called infinite-layer structure, where CuO_2 sheets made of corner-sharing CuO_4 squares alternate along the *c*-axis with Sr layers without oxygen. The infinite-layer structure was reported for the first time for $\text{Ca}_{1-x}\text{Sr}_x\text{CuO}_2$ with $x = 0.14$ prepared at ambient pressure (5), while we found that this structure can be stabilized for a wide compositional range of $A = \text{Ba}_{1/3}\text{Sr}_{2/3}$ to $\text{Sr}_{1/3}\text{Ca}_{2/3}$ if a high pressure of 6 GPa is used for synthesis (1). Smith *et al.* and Er *et al.* reported more recently their success in making this structure superconducting by partially substituting rare earth elements for Sr in SrCuO_2 (6, 7).

Though the usefulness of high-pressure treatments has thus been clearly shown, superconductors would be nothing but small

* To whom correspondence should be addressed.

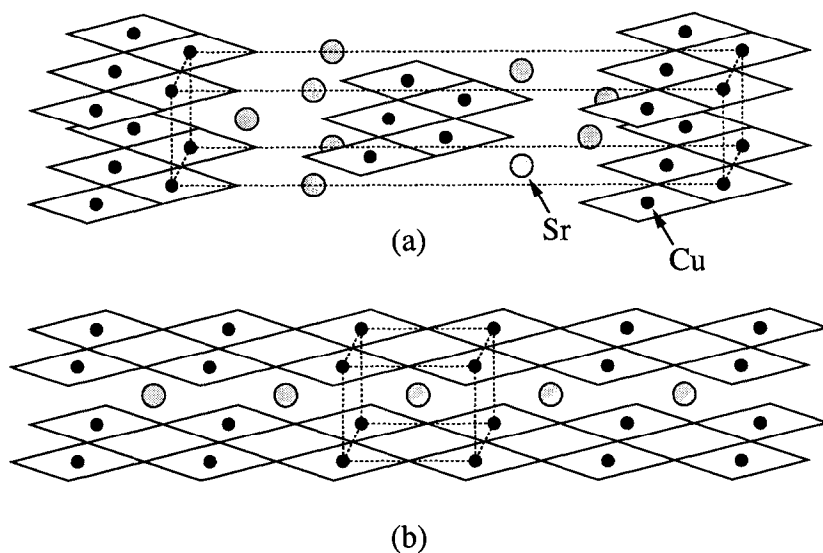


FIG. 1. Crystal structures of the low-pressure form (a) and the high-pressure form (b) of SrCuO₂.

visible peaks on icebergs of potentially interesting high-pressure phases. In studying the Sr–Cu–O system, we have found a new homologous series of compounds having a general formula of Sr_{*n*−1}Cu_{*n*+1}O_{2*n*} (*n* = 3, 5, . . . ∞). These are attractive because these contain a new type of Cu–O sheet.

Three compounds have been known in the Sr–Cu–O system studied at ambient pressure. They are Sr₂CuO₃, SrCuO₂ (8), and Sr₁₄Cu₂₄O₄₁ (9). All of them have as a common structural unit a planar CuO₄ square. In Sr₂CuO₃, CuO₄ squares share corners to form single chains, while SrCuO₂ contains Cu–O double chains bundled by edge-sharing (Fig. 1(a)). Sr₁₄Cu₂₄O₄₁ consists of two interpenetrating substructures, Cu₂O₃ sheets made of Cu–O double chains and Cu–O chains made of distorted CuO₄ squares sharing edges. In the case of SrCuO₂, pressure induces a structural transformation to the tetragonal infinite-layer structure with *a* = 3.926 and *c* = 3.432 Å (Fig. 1(b)). Specific density is higher by more than 7% in the high-pressure phase. On the Cu-rich side, the serial phases

Sr_{*n*−1}Cu_{*n*+1}O_{2*n*} (*n* = 3, 5, . . .) are formed; they do not exist at ambient pressure.

Experimental

Starting oxides having various Sr/Cu ratios were packed in gold capsules and compressed at 6 GPa in a belt-type high-pressure apparatus. Heat treatment under pressure was carried out at 1273 ~ 1573 K for 0.5 hr. The products were examined by powder X-ray diffraction (XRD), electron diffraction (ED), and high-resolution electron microscopy (HREM, JEM-2000EX equipped with a top-entry goniometer stage).

Results

The *n* = 5 phase (Sr₄Cu₆O₁₀) has an orthorhombic lattice of space group *Cmmm* with *a* = 3.931, *b* = 19.408, and *c* = 3.460 Å. The *a* and *c* values are almost the same as those of the tetragonal *n* = ∞ structure, while the *b*-axis is about 5 times as long as *a*. Figures 2(a) and (b) show HREM images and corresponding ED patterns, from which

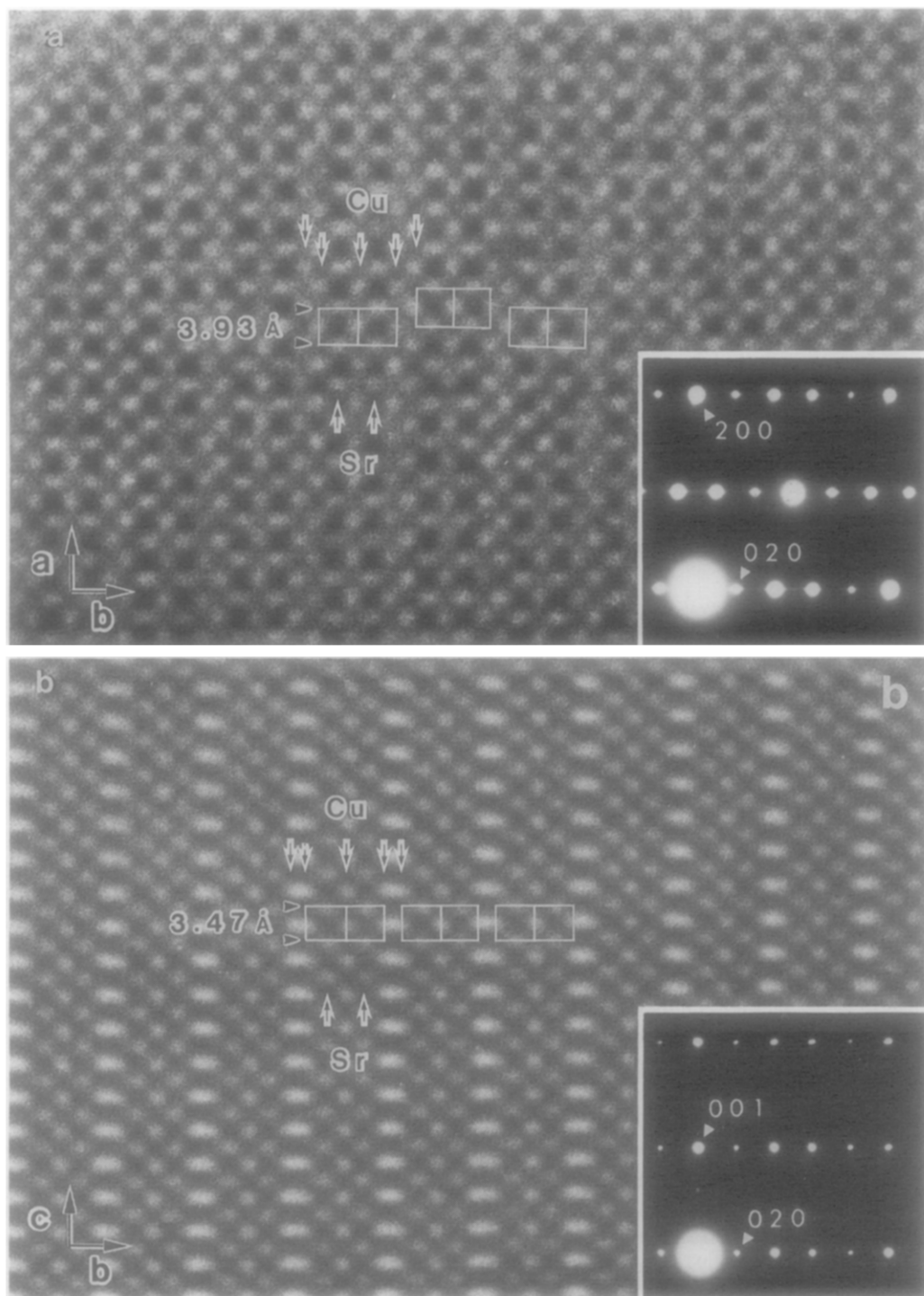


FIG. 2. High-resolution images and the corresponding ED patterns of the $n = 5$ phase taken with the incident electron beam along the c -axis (a) and the a -axis (b). The large and small black dots represent Sr and Cu atoms, respectively. Schematically illustrated in (c) is the $n = 5$ structure.

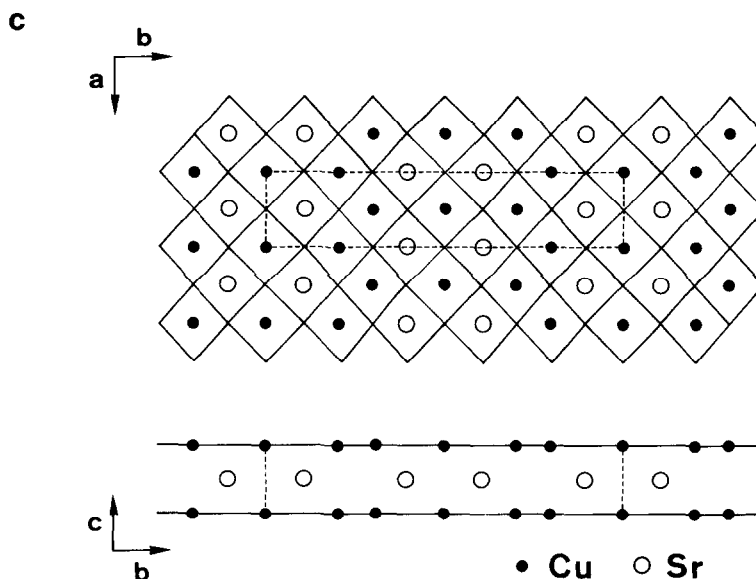


FIG. 2—Continued

its real-space structure can be very easily constructed, as illustrated in Fig. 2(c). Two kinds of black dots are identified clearly in the charge density map reflecting the in-plane structure, Fig. 2(a); the large one is a Sr atom and the small one a Cu atom. In further detail, two different crystallographic sites are seen for Cu; one within a double chain along the a -axis and the other between a pair of double chains. In Fig. 2(b), which shows a cross-sectional view of the layer stacking, the double Cu chain is seen as an elliptical dot because the b -axis component of the Cu–Cu distance within a double chain is only about 1.9 Å. It is evident that both kinds of Cu sites are within a plane sandwiched by Sr layers. As illustrated in Fig. 2(c), double and single Cu–O chains alternate with each other along the b -axis. The unit cell includes 4 Cu, 6 Sr, and 10 O atoms.

On the other hand, the $n = 3$ phase ($\text{Sr}_2\text{Cu}_4\text{O}_6$) has an orthorhombic unit cell of space group $Cmmm$ with dimensions of $a = 3.934$, $b = 11.573$, and $c = 3.495$ Å, where $b \sim 3a$. As seen from the HREM image in

Fig. 3(a), the Cu–O sheet is made of only Cu–O double chains without any bridging network, as shown in Fig. 3(b). This structure is similar to that of CaCu_2O_3 , but the Cu–O sheets in CaCu_2O_3 are strongly puckered (10). CaCu_2O_3 is formed under ambient pressure in the CaO–CuO system, while there is no corresponding phase in the SrO–CuO system at ambient pressure. The $n = 3$ and 5 phases were clearly identified by powder XRD, while those with larger n 's have been identified only by ED and HREM experiments as defects intergrown with the $n = 5$ phase. Figure 4 shows a typical intergrowth structure. In contrast with this, Cu–O double chains appear as planar defects in the infinite-layer structure in Fig. 5, which was obtained from a stoichiometric sample ($\text{Sr}/\text{Cu} = 1/1$) treated at 1323 K, where the infinite-layer structure becomes unstable.

The lattice parameters of these phases are listed in Table I. As n decreases, both a and c increase monotonically. The average size of the perovskite unit along the b -axis, b/n ,

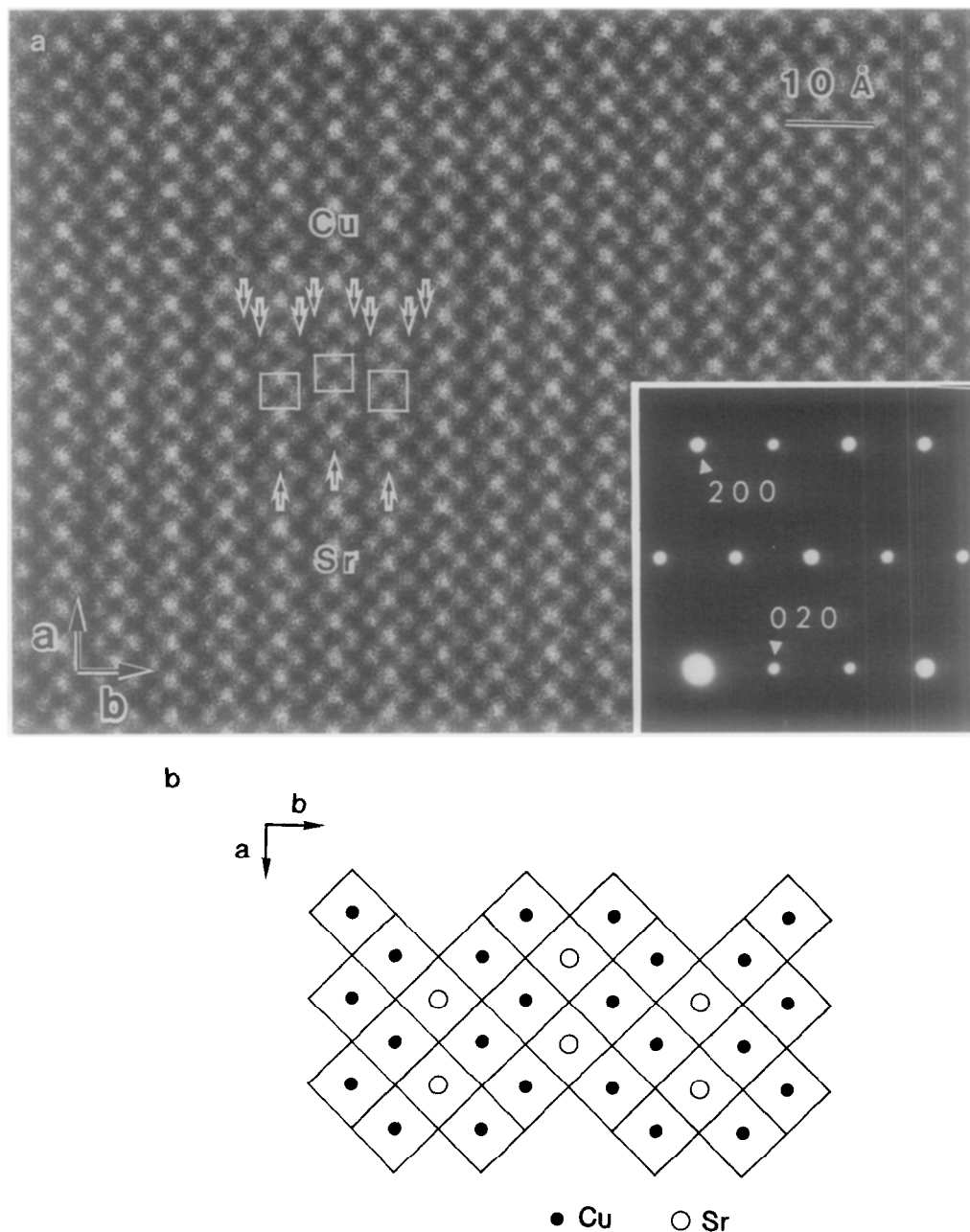


FIG. 3. HREM image of the $n = 3$ phase (a). The Cu-O sheet is made of only Cu-O double chains without any bridging CuO_4 network (b).

is smaller than a and decreases with decreasing n . This suggests that CuO_4 squares forming double chains are considerably con-

tracted along the b -axis. The contraction can directly be seen in HREM images like Figs. 2(a) and 3(a). The double chains in the

TABLE I
LATTICE PARAMETERS AND CALCULATED DENSITY OF
 $\text{Sr}_{n-1}\text{Cu}_{n+1}\text{O}_{2n}$ ($n = 3, 5$, AND ∞)

n	Formula	a (Å)	b (b/n) (Å)	c (Å)	V (Å ³)	Density (g/cm ³)
∞	SrCuO_2	3.926	3.926	3.432	52.899	5.750
5	$\text{Sr}_4\text{Cu}_6\text{O}_{10}$	3.931	19.408 (3.882)	3.460	263.973	5.610
3	$\text{Sr}_2\text{Cu}_4\text{O}_6$	3.934	11.573 (3.858)	3.495	159.121	5.483

low-pressure phase of SrCuO_2 and those in $\text{YBa}_2\text{Cu}_4\text{O}_8$ (11) are also deformed similarly. Denoting the O–Cu–O distance along the b -axis in a double chain and that in the edge-sharing CuO_4 network as a' and a'' , respectively, the lattice parameter b for the n phase can be expressed as

$$b = 3a' + (n - 3)a''.$$

a' of the $n = 3$ phase is given as $b/3 = 3.858$ Å, and a'' of the $n = 5$ phase as $(b - 3a')/2 = 3.918$ Å by assuming that a' is independent of n . Thus, the CuO_4 square is distorted by about 1.8% in the double chain, while it remains nearly regular in the edge-sharing CuO_4 network.

$2 = 3.918$ Å by assuming that a' is independent of n . Thus, the CuO_4 square is distorted by about 1.8% in the double chain, while it remains nearly regular in the edge-sharing CuO_4 network.

Discussion

It is well known that homologous series like $\text{Ti}_n\text{O}_{2n-1}$, $\text{Mo}_n\text{O}_{3n-1}$, and $\text{W}_n\text{O}_{3n-2}$ possess shear structures (12). These serial com-

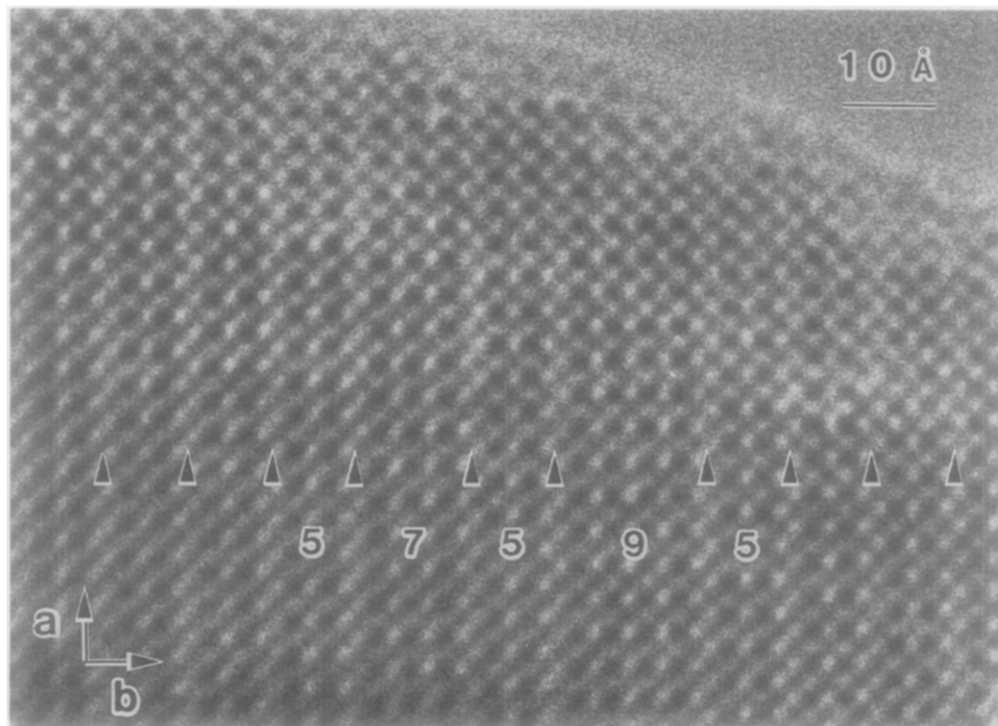


FIG. 4. Intergrowth of phases with various n 's seen within the ab -plane.

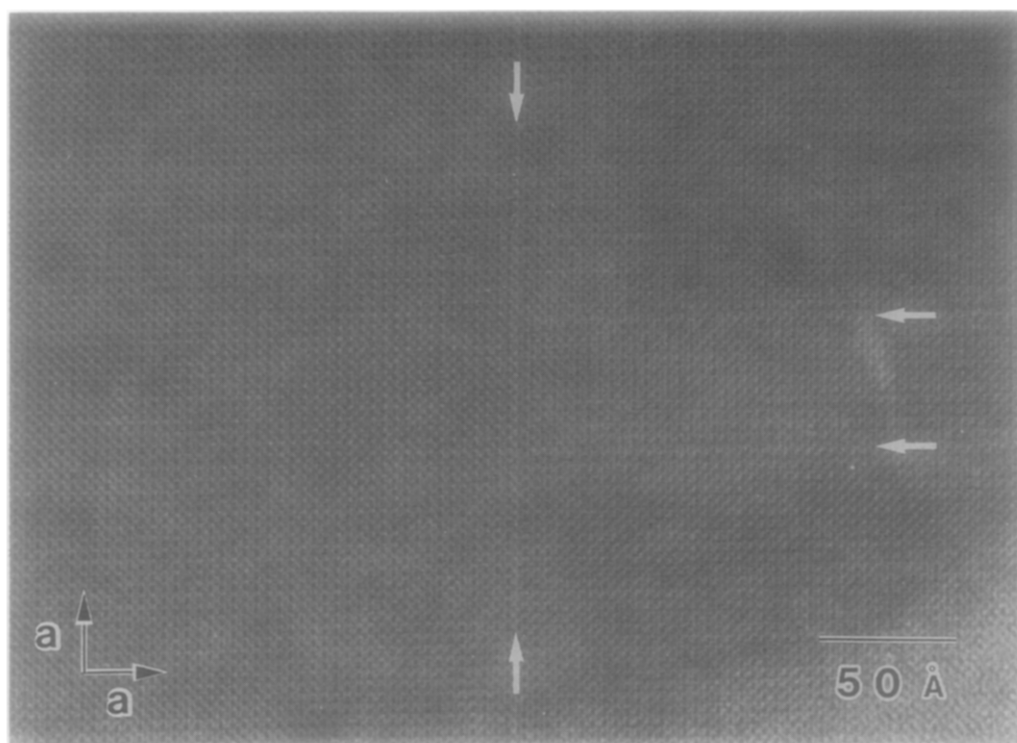


FIG. 5. Electron micrograph obtained from a Sr/Cu = 1/1 sample treated at 1323 K. Cu-O double chains appear, in this case, as planar defects as marked by arrows in the infinite-layer structure.

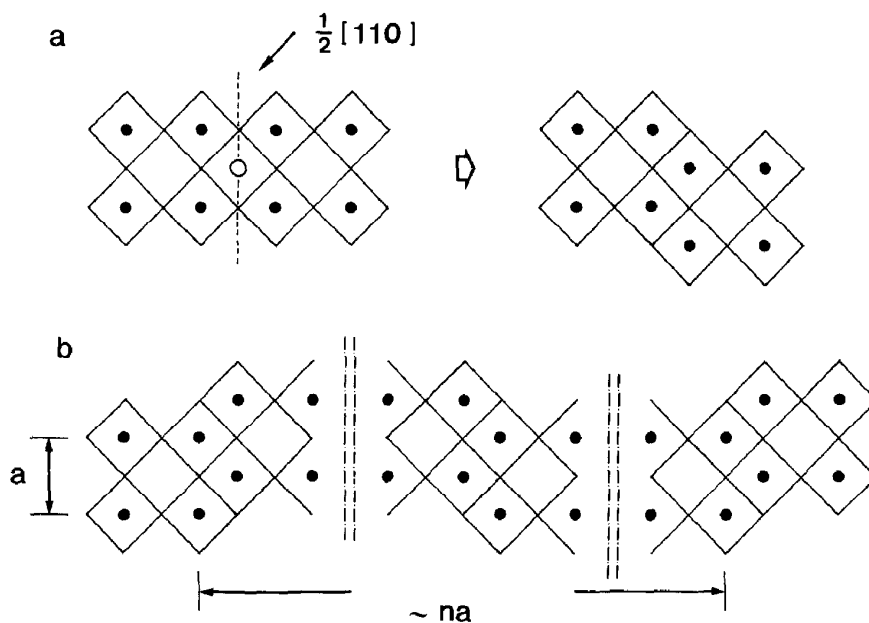


FIG. 6. Shear process forming Cu-O double chains in the parent $n = \infty$ structure of SrCuO_2 (a). The resulting orthorhombic unit cell has a $b \sim na$ (b).

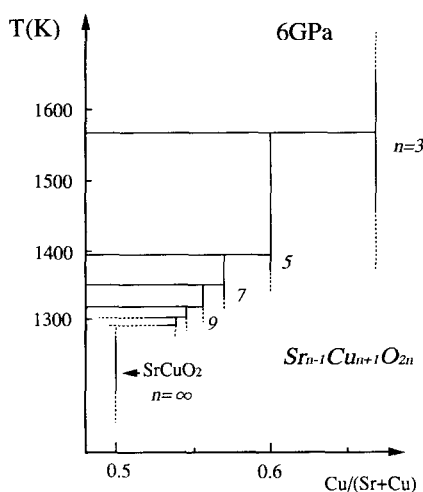


FIG. 7. Tentative phase diagram of the SrO-CuO system under high pressure, 6 GPa. The title series of phases with smaller n 's tend to be stabilized at higher temperatures.

positions depend upon the indices of the shear planes and upon the frequency of shearing. The present system can also be understood in the same manner. Figure 6(a) illustrates the relevant shear process. Starting from the parent $n = \infty$ structure, one double Cu-O chain is created after shearing with a shear vector of $\langle 110 \rangle / 2$. The resulting orthorhombic unit cell with $b \sim na$ including

two double chains is illustrated in Fig. 6(b). The composition is given by subtracting two SrO units from $(n + 1)\text{SrCuO}_2$ as follows:



n needs to be odd if the distance between neighboring double chains is unique.

A tentative phase diagram of the SrO-CuO system under high pressure, 6 GPa, is depicted in Fig. 7. The infinite-layer structure of SrCuO_2 becomes unstable above ca. 1300 K. The homologous series of $\text{Sr}_{n-1}\text{Cu}_{n+1}\text{O}_{2n}$ exist on the Cu-rich side. Those with smaller n 's tend to be stabilized at higher temperatures. On the other hand, two phases appear on the Cu-poor side which are not shown in the figure, Sr_2CuO_3 ($T > 1500$ K) and an unidentified phase with a tetragonal lattice of $a = 3.92$ and $c = 10.92$ Å ($T < 1500$ K).

Physical properties of the homologous phases are under investigation. Since there are no oxygen ions between the Cu-O sheets, electrical and magnetic properties must be strongly two-dimensional. It is interesting to notice that the intersection by double chains causes an antiferromagnetic frustration; one possible spin structure is shown in Fig. 8. It is quite reasonable to assume that antiferromagnetic interactions

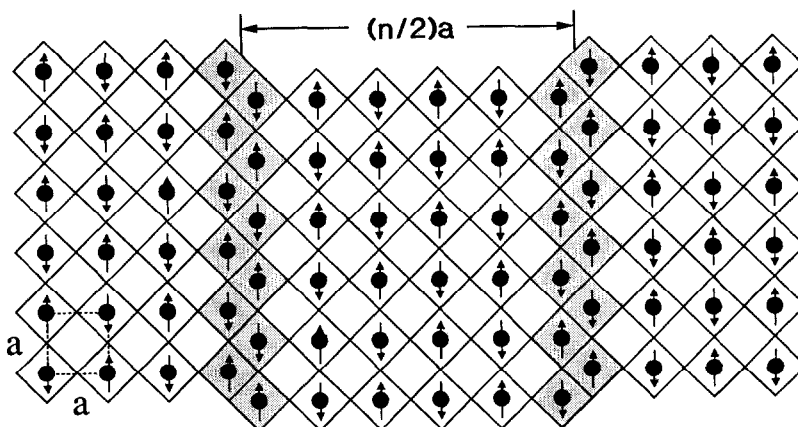


FIG. 8. Possible spin structure of $\text{Sr}_{n-1}\text{Cu}_{n+1}\text{O}_{2n}$. The intersection of the normal CuO_2 sheets by double chains causes an antiferromagnetic frustration.

are dominant along linear Cu–O–Cu bonds. Then, there occurs a frustration in the spin arrangement within the double chains locally. These phases can be expected to remain antiferromagnetically short-range ordered down to very low temperatures. Though large- n phases were not isolated in the present study, we are sure that use of more appropriate starting materials and more suitable heating conditions makes it possible in the near future.

In conclusion, we have clarified the formation of $\text{Sr}_{n-1}\text{Cu}_{n+1}\text{O}_{2n}$ ($n = 3, 5, \dots, \infty$) under high pressure. They offer a new type of Cu–O sheet within which an antiferromagnetic frustration can be expected.

Acknowledgments

This work was partly supported by Grants-in-Aid for Scientific Research on Priority Areas, "Mechanism of Superconductivity" and "Chemistry of New Superconductors," from the Ministry of Education, Science, and Culture.

References

1. M. TAKANO, Y. TAKEDA, H. OKADA, M. MIYAMOTO, AND K. KUSAKA, *Physica C* **159**, 375 (1989).
2. H. OKADA, M. TAKANO, AND Y. TAKEDA, *Physica C* **166**, 111 (1990).
3. M. TAKANO, M. AZUMA, Z. HIROI, Y. BANDO, AND Y. TAKEDA, *Physica C* **176**, 441 (1991).
4. Z. HIROI, M. TAKANO, M. AZUMA, Y. TAKEDA, AND Y. BANDO, to be published.
5. T. SIEGRIST, S. M. ZAHURAK, D. W. MURPHY, AND R. S. ROTH, *Nature (London)* **334**, 231 (1988).
6. M. G. SMITH, A. MANTHIRAM, J. ZHOU, J. B. GOODENOUGH, AND J. T. MARKERT, *Nature (London)* **351** 549 (1991).
7. G. ER, S. KIKAWA, F. KANAMARU, AND Y. MIYAMOTO, to be published.
8. C. L. TESKE AND H. K. MULLER-BUSCHBAUM, *Z. Anorg. Allg. Chem.* **371**, 325 (1969); **379**, 234 (1970).
9. T. SIEGRIST, L. F. SCHNEEMEYER, S. A. SUNSHINE, AND J. V. WASZCZAK, *Mater. Res. Bull.* **23**, 1429 (1988).
10. C. L. TESKE AND H. K. MULLER-BUSCHBAUM, *Z. Anorg. Allg. Chem.* **370**, 134 (1969).
11. P. FISHER, J. KARPINSKI, E. KALDIS, E. JILEK, AND S. RUSIECKI, *Solid State Commun.* **69**, 531 (1989).
12. A. D. WADSLEY, "Non-stoichiometric Compounds," p. 98, Academic Press, New York (1968).